AIAA JOURNAL
Vol. 37, No. 6, June 1999

# Shapes of Nonbuoyant Round Luminous Laminar-Jet Diffusion Flames in Coflowing Air

K.-C. Lin* and G. M. Faeth†
*University of Michigan, Ann Arbor, Michigan 48109-2140*

**The shapes (luminous flame boundaries) of steady nonbuoyant round luminous hydrocarbon-fueled laminar-jet diffusion flames burning in coflowing air were studied both experimentally and theoretically. Flame shapes were measured from photographs of flames burning at low pressures in order to minimize the effects of buoyancy. Test conditions involved acetylene-, propylene- and 1,3-butadiene-fueled flames having initial reactant temperatures of 300 K, ambient pressures of 19–50 kPa, jet-exit Reynolds numbers of 18–121, and initial air/fuel velocity ratios of 0.22–32.45 to yield luminous flame lengths of 21–108 mm. The present flames were close to the laminar smoke point but were not soot emitting. Simple expressions to estimate the shapes of nonbuoyant laminar-jet diffusion flames in coflow were found by extending an earlier analysis of Mahalingam et al. (Mahalingam, S., Ferziger, J. H., and Cantwell, B. J., "Self-Similar Diffusion Flames," *Combustion and Flame*, Vol. 82, No. 2, 1990, pp. 231–234). These formulas provided a good correlation of present measurements except near the burner exit where self-similar approximations used in the simplified analysis are no longer appropriate.**

## Nomenclature

| | |
|---|---|
| $C_f$ | = empirical flame length factor |
| $D$ | = mass diffusivity |
| $d$ | = jet-exit diameter |
| $Fr_a$, $Fr_f$ | = air and fuel stream Froude numbers, $u_{a,o}^2/(2gL_f)$ and $u_{f,o}^2/(2gL_f)$ |
| $f$ | = mixture fraction |
| $g$ | = acceleration of gravity |
| $L_f$ | = distance from jet exit to luminous flame tip |
| $L_o$ | = distance from jet exit to virtual origin |
| $\dot{m}$ | = burner mass flow rate |
| $p$ | = pressure |
| $Re$ | = jet Reynolds number, $4\dot{m}/(\pi d\mu)$ |
| $r$ | = radial distance |
| $Sc$ | = Schmidt number, $\nu/D$ |
| $u$ | = streamwise velocity |
| $u_d$ | = streamwise velocity defect; Eq. (1) |
| $w$ | = luminous flame diameter |
| $w_{\frac{1}{2}}$ | = luminous flame diameter at $\zeta = \frac{1}{2}$ |
| $x$ | = streamwise distance |
| $Y_{\text{FUEL}}$ | = mass fraction of fuel |
| $Y_{\text{OXYGEN}}$ | = mass fraction of oxygen |
| $Z_{\text{st}}$ | = stoichiometric mixture fraction |
| $\zeta$ | = normalized streamwise distance; Eq. (12) |
| $\eta$ | = dimensionless radial distance; Eq. (6) |
| $\mu$ | = dynamic viscosity |
| $\nu$ | = kinematic viscosity |
| $\rho$ | = density |
| $\sigma_i$ | = standard deviation of parameter $i$ |

*Subscripts*

| | |
|---|---|
| $a$ | = airstream property |
| $f$ | = fuel-stream property |
| $o$ | = burner exit-plane condition |

## Introduction

LAMINAR nonpremixed (diffusion) flames are of interest because they provide model flame systems that are far more tractable for analysis and experiments than more practical turbulent diffusion flames. Certainly understanding flame processes within laminar-jet diffusion flames must precede understanding these processes in more complex turbulent diffusion flames. In addition, many properties of laminar-jet diffusion flames are directly relevant to turbulent diffusion flames using laminar flamelet concepts.[1] Laminar-jet diffusion flame shapes (luminous flame boundaries) have been of particular interest since the classical study of Burke and Schumann[2] because they are a simple nonintrusive measurement that is convenient for evaluating flame-structure predictions. Motivated by these observations, the shapes of laminar diffusion flames were considered during the present investigation.

Nonbuoyant flames were emphasized during the present investigation to simplify interpretation and analysis of the measurements and increase the relevance of the results because most practical flames are not buoyant. Effects of buoyancy were minimized by observing flames having large flow velocities at small pressures.[3] Present methods were based on the study of the shapes of nonbuoyant round laminar-jet diffusion flames in still air due to Lin et al.,[4] who found that a simple analysis due to Refs. 5 and 6 yielded good predictions of the flame shapes reported by Urban et al.[7] and Sunderland et al.[8,9] The objective of the present study was to extend Ref. 4 to consider the shapes of nonbuoyant round laminar-jet diffusion flames in coflowing air, prompted by the widespread use of this configuration to study the structure and soot formation processes of laminar diffusion flames (see Refs. 10–19 and references cited therein). Similar to Ref. 4, a way to correlate flame-shape results was sought, convenient for use by others, based on simplified analysis of nonbuoyant laminar coflowing jet diffusion flames.

Most earlier studies of the shapes of nonbuoyant laminar-jet diffusion flames considered round hydrocarbon-fueled flames burning in still gases (generally air) (see Refs. 4–8, 20–33, and references cited therein). The results of these studies have raised several concerns: what conditions are needed to minimize effects of buoyancy when observations of nonbuoyant flames are sought at normal gravity, what is the effect of transient flame development on flame-shape measurements when nonbuoyant conditions are provided by ground-based facilities where available test times are limited, and what is the effect of soot luminosity on the flame-shape measurements of hydrocarbon-fueled flames?[7] With respect to minimizing effects of buoyancy at normal gravity, experiments at low pressures[3] and with very large flow velocities[33] have proven to be effective tactics that will be exploited during the present study. Transient flame development effects have been problematical using ground-based low-gravity facilities due to the limited test times of drop towers[24–27] and the flight-path disturbances of aircraft facilities.[7–9] Recent measurements from long-term low-gravity tests in space[7]

Received Aug. 20, 1998; revision received Dec. 15, 1998; accepted for publication Jan. 7, 1999. 

*Research Associate, Department of Aerospace Engineering; currently Research Scientist, Taitech, Inc., Wright–Patterson Air Force Base, OH 45433-0630.

†A. B. Modine Professor, Department of Aerospace Engineering. Fellow AIAA.

and drop-tower tests at reduced pressures,[8] however, have minimized transient flame development problems and yielded results that could be correlated by simplified theories as mentioned earlier.

Effects of soot luminosity on the shapes of hydrocarbon-fueled laminar-jet diffusion flames in still air are more problematical than effects of buoyancy and transient flame development. The luminosity of hydrocarbon-fueled flames is caused mainly by glowing soot particles; therefore, the relationships between luminous flame dimensions and the location of the flame sheet (where the local mixture fraction is stoichiometic) are the main issues because the latter is generally associated with predictions of laminar flame shapes. Past measurements of the structure and soot properties of weakly buoyant and buoyant round laminar-jet diffusion flames burning in still or slowly moving air indicate that luminous/stoichiometric flame-length ratios are in the range 0.9–1.8, with the largest values observed as the laminar smoke point (the condition where the flame first begins to emit soot) is approached.[9,12–16] This behavior occurs because soot oxidation begins at slightly fuel-rich conditions and can continue in the fuel-lean region for a time before the soot is either consumed (for non-soot-emitting or nonsooting flames) or the soot oxidation reactions are quenched (for soot-emitting or sooting flames), with luminous flame lengths varying accordingly.[9] Finally, recent measurements of nonbuoyant laminar-jet diffusion flames in still air show that luminous flame lengths near laminar smoke-point conditions are roughly twice as long as those of soot-free (blue) flames at comparable conditions.[4,8] Fortunately, flame shapes at these two limiting conditions could still be correlated effectively based on the simplified Spalding[5] analysis, after defining an empirical factor to represent effects of soot luminosity.[4] Such empiricism is not desirable, but it is unavoidable at the present time because of limited understanding about soot reaction processes.

Even though the classic study of Burke and Schuman[2] addressed the shapes of laminar coflowing jet diffusion flames (for the limiting condition where initial fuel and oxidant velocities were the same), there has been relatively little subsequent consideration of this problem. Exceptions include the theoretical studies of Williams[34] and Mahalingam et al.,[35] which extended the Burke and Schumann[2] analysis to treat flames where the outer coflowing stream was unbounded. During the present study, the simple self-similar analysis of Mahalingam et al.[35] was further developed to provide a theoretical basis for correlating the shapes of nonbuoyant laminar-jet diffusion flames in coflowing air, analogous to the use of the simplified analysis of Spalding[5] to provide a theoretical basis for correlating the shape of nonbuoyant laminar-jet diffusion flames in still air by Lin et al.[4]

The preceding discussion suggests that significant progress has been made concerning the shapes of the hydrocarbon-fueled laminar-jet diffusion flames in still air but that corresponding information for flames in coflowing air is very limited in spite of the importance of this configuration for studies of soot processes in laminar-jet diffusion flames. With this status in mind, the present investigation considered nonbuoyant round luminous laminar-jet diffusion flames in coflowing air with the following specific objectives:

1) Measure the shapes (luminous flame boundaries) and associated properties such as laminar flame lengths and diameters for various fuel types, coflow velocities, jet-exit flow rates and ambient pressures.

2) Compare present measurements with earlier findings for similar flames in still air, e.g., the flames observed in Ref. 4, to help quantify effects of coflow on flame-shape properties.

3) Exploit the new measurements to develop a correlation for the shapes of coflowing laminar-jet diffusion flames, convenient for use by others, by extending the earlier analysis of Burke and Schumann[2] flames due to Mahalingam et al.[35]

Present observations were limited to soot-containing acetylene-, propylene- and 1,3-butadiene-fueled laminar-jet diffusion flames burning in coflowing air. Similar to Ref. 4, the measurements were limited to conditions near the laminar smoke point except for some preliminary observations to study the effect of approach to the laminar smoke point on flame shapes.

The following discussion begins with descriptions of experimental and theoretical methods. Results are then considered, treating flame appearance, luminous flame lengths, luminous flame diameters, and luminous flame shapes, in turn. Major conclusions are summarized at the end of the paper.

## Experimental Methods

Experimental methods will be described only briefly (see Refs. 17–19 for more details). Effects of buoyancy were minimized by observing flames at relatively small pressures ($\leq$50 kPa) with either relatively large coflow velocities (air/fuel velocity ratios up to 32.45) or relatively large source Froude numbers when coflow velocities were small. The burner was placed within a windowed cylindrical chamber and directed vertically upward along its axis. The burner was a coaxial-tube arrangement with the fuel flowing from the inner port (6-mm inside diameter with the tube wall tapered to provide a negligible thickness at the tube exit) and air flowing from a concentric outer port (60-mm inside diameter). The inner port had sufficient length to provide fully developed laminar pipe flow at the burner exit. The outer port had several layers of beads and screens to provide a uniform velocity flow at the burner exit. Flame lengths were limited so that test conditions approximated flames in a uniform air coflow based on laser velocimetry measurements of flow velocity distributions.[17,19] The windowed chamber had a diameter of 300 mm and a length of 1200 mm. Optical access was provided by two pairs of opposing windows having diameters of 100 mm and centered on a horizontal plane located 500 mm above the base of the windowed chamber. The flames were positioned so that their full lengths could be observed and photographed through the windows.

Fuel was supplied to the inner port from commercial gas cylinders. Fuel flow rates were controlled and metered with critical flow orifices in conjunction with pressure regulators with this system calibrated with wet-test meters. Air was supplied from the room using critical flow orifices to control and meter air-flow rates. The exhaust products passed through a porous plate into a plenum chamber at the top of the windowed chamber to provide uniform flow conditions in the vicinity of the test flame. After dilution with air to reduce flow temperatures, the exhaust flow was removed using the laboratory vacuum pump system. The flames were ignited by a hot wire that could be manually moved out of the flowfield once flame stabilization was complete.

Dark field photographs of the flames were obtained using a 35-mm reflex camera. The photographs were subsequently printed using a 100 × 125 mm film format. The flames were measured directly from these prints, using photographs of objects of known size to calibrate vertical and horizontal distances on the prints. Experimental uncertainties (95% confidence) of luminous flame diameters and lengths were less than 2 and 5%, respectively.

Present test conditions are summarized in Table 1. Gas purities were greater than 99% for propylene and 1,3-butadiene but were only roughly 98% for acetylene due to contamination by acetone that is present in commercial acetylene gas cylinders for safety purposes. The effect of the acetone was evaluated by comparing observations with and without acetone vapor present, using the acetone purification system described by Hamins et al.[36] to create the acetone-free fuel stream. The effect of acetone on luminous flame shapes (and laminar smoke-point flame lengths[17,19]) was small compared with experimental uncertainties. Present test conditions included reactant

**Table 1 Summary of test conditions[a]**

| Parameter | Acetylene | Propylene | 1,3-Butadiene |
|---|---|---|---|
| Fuel flow rate, mg/s[b] | 0.94–5.90 | 1.53–4.08 | 0.74–2.71 |
| $Re$ (−) | 19–121 | 38–101 | 18–66 |
| $u_{a,o}/u_{f,o}$ (−) | 0.22–12.03 | 0.29–6.99 | 0.77–32.45 |
| $\mu_{fo}$, mg/s-m | 10.3 | 8.61 | 8.66 |
| $L_f$, mm | 21–108 | 41–108 | 21–75 |
| $w_{1/2}$, mm | 3.5–9.5 | 5.9–13.1 | 4.3–10.0 |
| $Z_{st}$ | 0.0704 | 0.0636 | 0.0667 |

[a]Fuel port inside diameter of 6 mm and concentric air port inside diameter of 60 mm with burner directed vertically upward. Reactant temperatures of roughly 300 K with ambient pressures of 19–50 kPa.

[b]Commercial grade gases in cylinders with purities as follows: greater than 98.0% for acetylene and greater than 99.0% for propylene and 1,3-butadiene.

temperatures of roughly 300 K, ambient pressures of 19–50 kPa, jet-exit Reynolds numbers of 18–121, and initial air/fuel velocity ratios of 0.22–32.45.

## Theoretical Methods

The objective of the analysis was to develop a convenient way to help interpret and correlate flame-shape measurements for nonbuoyant laminar-jet diffusion flames in coflowing air, analogous to the approach used by Lin et al.[4] for the shapes of nonbuoyant laminar-jet diffusion flames in still air. Thus, a set of easily used equations was sought, along with recommendations for selecting the thermochemical and transport properties appearing in these equations, as opposed to more complete methods that would require numerical solutions on a computer. The approach used was to extend the analysis of Mahalingam et al.[35] (which considers the Burke and Schumann[2] problem in the self-similar regime far from the source when the outer reactant stream is unbounded) to treat the present problem. The following description of the analysis is brief. A more detailed example of this general approach, for somewhat different initial conditions and property assumptions, is provided by Mahalingam et al.[35]

Except for changed ambient flow properties, the major assumptions of the present flame-shape analysis are similar to those used earlier by Lin et al.[4] as follows: 1) Attention is limited to steady, axisymmetric laminar-jet diffusion flames burning at constant pressure in an unbounded coflowing gas having uniform properties; 2) effects of buoyancy and associated changes of potential energy are negligible; 3) the Mach number of the flow is small so that effects of viscous dissipation and changes of kinetic energy can be ignored; 4) the flame has a large aspect ratio so that diffusion of mass (species), momentum, and energy in the streamwise direction is small; 5) for the same reasons, the solution of the governing equations can be approximated by far-field conditions where the details of initial conditions can be replaced by integral invariants of the flow for the conservation of mass, momentum, and energy; 6) all chemical reactions occur in a thin-flame sheet with fast chemistry so that fuel and oxidant are never simultaneously present at finite concentrations; 7) the diffusivities of mass (of all species), momentum, and energy are all equal; 8) all thermophysical and transport properties are constant throughout the flame; and 9) effects of radiation are small. The first three assumptions are justified as conditions of the present experiments. The fourth and fifth assumptions are justified for most of the present measurements that have large aspect ratios, e.g., the present measurements summarized in Table 1 have flame aspect ratios $2L_f/w_{1/2}$ in the range 4–62 and burner aspect ratios $2L_f/d$ in the range 7–36. The sixth assumption, prescribing a thin-diffusion flame sheet, has a long history of effective use to find the shapes of laminar-jet diffusion flames, dating back to Burke and Schumann.[2] The remaining assumptions, however, are not satisfied by laminar-jet diffusion flames and were only adopted so that simple flame-shape formulas could be found, based on the past success of similar approximations to find the shapes of laminar-jet diffusion flames (see Refs. 4–8, 28–31, and references cited therein).

The flame configuration and notation used for the present analysis is sketched in Fig. 1. The approach is limited to self-similar behavior far from the source so that the details of source properties are not important; therefore, the source is represented by uniform average fuel- and air-stream velocities $u_{f,o}$ and $u_{a,o}$. The mixture fractions (defined as the fraction of mass at a point that originated from the source fuel stream) of the source fuel and air streams are $f_{f,o} = 1$ and $f_{a,o} = 0$ by definition. The enthalpy defect of the source can be defined in an analogous way, but this is not necessary because conservation of energy principles are not needed to find flame shapes under the present assumptions. The streamwise velocity defect is defined as follows:

$$u_d = u_{a,o} - u \tag{1}$$

noting that the airstream velocity approaches $u_{a,o}$ at large $r$ for all distances from the source, based on assumption (1). In the far field, where self-similar behavior is approached, $|u_d|/u_{a,o} \ll 1$ (the absolute value is used to allow for values of $u_{f,o}$ both larger and smaller than $u_{a,o}$) and quadratic and higher terms in $u_d$ can be neglected in the governing equations. Then, under the present approximations,

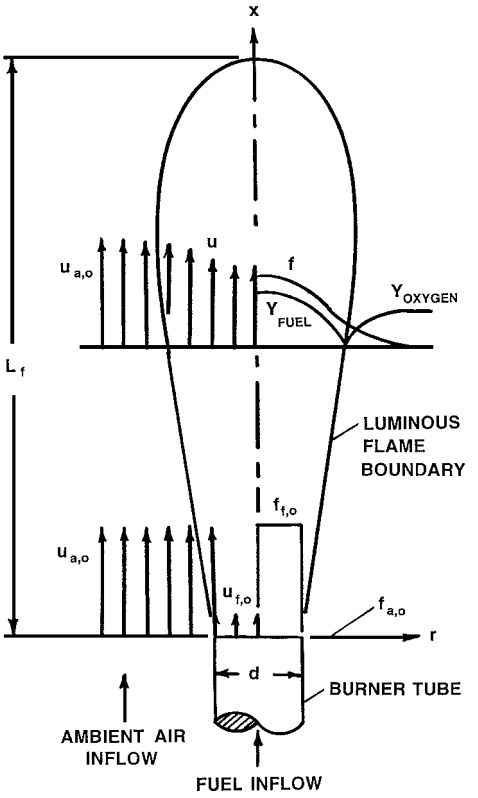


**Fig. 1 Sketch of the coflowing laminar-jet diffusion flame configuration.**

the governing equation for conservation of mixture fraction can be found in the same manner as the far-field formulation of laminar wake processes, as follows[37]:

$$u_{a,o}\frac{\partial f}{\partial x} = \frac{\nu}{r}\frac{\partial}{\partial r}\left(r\frac{\partial f}{\partial r}\right) \tag{2}$$

$$r = 0: \quad \frac{\partial f}{\partial r} = 0, \qquad r \to \infty: \quad f = 0 \tag{3}$$

The final condition of the analysis is conservation of the flow of fuel-stream mass in the streamwise direction, which can be written as follows in far field:

$$\int_0^\infty f r\,\mathrm{d}r = \frac{\mathrm{d}^2 u_{f,o}}{8u_{a,o}} \tag{4}$$

The solution of Eqs. (2–4) can be obtained using either conventional separation of variables or conversion into an ordinary differential equation by a suitable similarity transformation.[37] The resulting expression for the mixture fraction distribution in the self-similar regime is as follows:

$$f = u_{f,o}\,\mathrm{d}^2 \exp\{-\eta^2\}/(16\nu x) \tag{5}$$

where

$$\eta = (r/2)[u_{a,o}/(\nu x)]^{\frac{1}{2}} \tag{6}$$

The location of the luminous flame boundary is assumed to coincide with the location of the thin flame sheet where the concentrations of fuel and oxidant are zero (see Fig. 1) and the stoichiometric mixture fraction is reached, $f = Z_{st}$ (see Table 1 for present values of $Z_{st}$). Introducing this mixture fraction into Eq. (5), for conditions along the flame axis, yields the following expression for luminous flame length:

$$\frac{L_f}{d} = \frac{Re}{16Z_{st}} \tag{7}$$

The corresponding expression for flame shape, providing the flame diameter as a function of streamwise distance, is as follows:

$$w/d = [(x/L_f)(u_{f,o}/u_{a,o})\,\ln\{L_f/x\}/Z_{st}]^{\frac{1}{2}} \tag{8}$$

Finally, a convenient measure of the flame diameter is its value at $x/L_f = \frac{1}{2}$, as follows:

$$w_{\frac{1}{2}}/d = [(u_{f,o}/u_{a,o})\, ln\{2\}/(2Z_{st})]^{\frac{1}{2}} \quad (9)$$

Correlation of the measurements was sought in the same manner as Lin et al.[4]: The equal diffusivity approximation was relaxed by introducing the Schmidt number into Eq. (7); the Schmidt number and viscosity used to compute the Reynolds number were taken from the properties of air at the average of the adiabatic flame temperature and the ambient temperature; the correlation of flame length was improved at small aspect ratios by introducing a virtual origin at a distance $L_o$ from the jet exit; and the flame length correlation was fine-tuned for effects of soot luminosity, etc., by introducing an empirical coefficient $C_f$ as discussed later. With these changes, Eq. (7) for the luminous flame length becomes

$$\frac{(L_f - L_o)}{d} = \frac{C_f ReSc}{16Z_{st}} \quad (10)$$

whereas Eq. (8) for the luminous flame diameter becomes

$$w/d = [-\zeta(u_{f,o}/u_{a,o})\, ln\{\zeta\}/Z_{st}]^{\frac{1}{2}} \quad (11)$$

where

$$\zeta = \frac{(x - L_o)}{(L_f - L_o)} \quad (12)$$

Equations (9–12) disclose some interesting properties of nonbuoyant laminar-jet diffusion flames in a coflowing and unbounded environment. First of all, the flame length from Eq. (10) is independent of the coflow velocity, which is surprising; nevertheless, flame lengths in still gases from Ref. 4 are a fixed ratio longer than in coflow (given similar values of $C_f$ and $L_o/d$), e.g., the coefficients in the flame-length expressions for still and coflowing gases are $\frac{3}{32}$ and $\frac{1}{16}$, respectively. Diameters of flames in coflow vary with the ratio $u_{f,o}/u_{o,a}$; in contrast, diameters of flames in still gases are independent of reactant flow rates.[4] Flame-diameter properties in both coflowing and still gases, however, are only indirectly affected by assumed transport properties through the computation of flame-length from Eq. (10). Finally, the present analysis agrees with the results of Mahalingam et al.[35] at their limiting Burke and Schumann[2] condition of $u_{f,o} = u_{a,o}$, except for the presence of the virtual origin and the different treatment of transport properties. The corresponding agreement between the self-similar prediction and the more exact Burke and Schumann[2] analysis for $u_{f,o} = u_{a,o}$ as the diameter of the outer reactant stream becomes large also is quite good in the far field, as discussed by Mahalingam et al.[35]

## Results and Discussion

### Flame Appearance

Photographs of acetylene-, propylene- and 1,3-butadiene-fueled flames are illustrated in Fig. 2 for comparable flow conditions (*Re* of 62–66 and $u_{a,o}/u_{f,o}$ of 3.3–4.2). All three flames are close to their laminar smoke points, which can be arranged because flame shapes are relatively independent of the ambient pressure, whereas

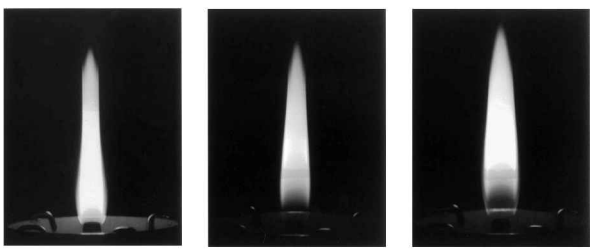


**Fig. 2 Photographs of acetylene-, propylene-, and 1,3-butadiene-fueled laminar-jet diffusion flames burning in coflowing air at similar air/fuel velocity ratios.**

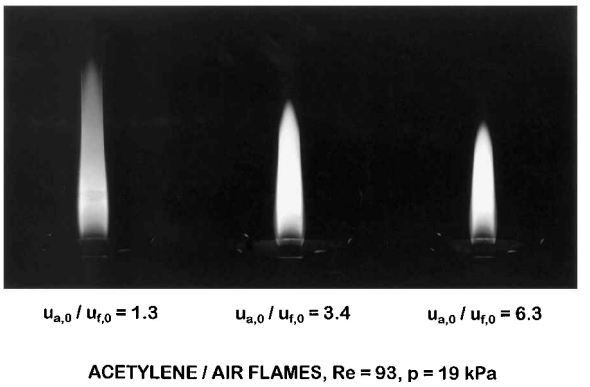


**Fig. 3 Photographs of acetylene-fueled laminar-jet diffusion flames burning in coflowing air at various air/fuel velocity ratios.**

laminar smoke-point flame lengths increase rapidly as the ambient pressure is decreased.[9] The 1,3-butadiene flame seems somewhat longer than the rest, but this is mainly because of the flame attachment farther downstream from the burner exit than the rest. Actually, all three flames have roughly the same length, which is consistent with Eq. (10) in view of the relatively small variation of $Z_{st}$ for these fuels (see Table 1) and past experience concerning the effect of approach to the laminar smoke point on luminous flame shapes from Lin et al.[4] Observed flame diameters are somewhat larger for the 1,3-butadiene-fueled flame than the rest, rather than being nearly the same as anticipated from Eq. (9). This level of discrepancy between measured and predicted flame diameters is typical of observations over the test program and is similar to past experience for flames in still gases from Lin et al.[4] In view of the simplicity of the flame-shape analysis, and the fact that average properties and empirical factors cannot be chosen to fit predictions and measurements of flame diameters, it is rather remarkable that the trends of flame-diameter predictions are still reasonably good.

Photographs of acetylene-fueled flames at given fuel jet-exit conditions and ambient pressures (*Re* of 93 and ambient pressure of 19 kPa) are illustrated in Fig. 3 for various air/fuel velocity ratios. Contrary to the expectations of Eq. (10), where luminous flame lengths are independent of air/fuel velocity ratio, the flame lengths illustrated in Fig. 3 decrease significantly as the air/fuel velocity ratio is increased. This behavior follows because luminous flame lengths progressively increase relative to soot-free (blue) flames at comparable conditions as laminar smoke-point conditions are approached. For example, the luminous flame lengths at the laminar smoke point are roughly twice as long as corresponding blue flames for nonbuoyant laminar-jet diffusion flames in still air,[4] and similar behavior is quite reasonable for flames in coflowing air. In particular, increasing air/fuel velocity ratios tend to increase laminar smoke-point flame lengths based on measurements of Lin and Faeth.[19] Thus, for $u_{a,o}/u_{f,o} = 1.3$ in Fig. 3 the flame has nearly reached its laminar smoke-point flame length of 60 mm, but for $u_{a,o}/u_{f,o} = 3.4$ the luminous flame length is only 50 mm compared to a laminar smoke-point flame length of roughly 110 mm for this air/fuel velocity ratio, which implies a flame length between the length of a soot-free (blue) flame and the length at the laminar smoke point. In view of this effect of approach to the laminar smoke point, the following flame-shape measurements were obtained near laminar smoke-point conditions, and the corresponding lengths of soot-free (blue) flames are likely to be much shorter.

### Flame Lengths

Luminous flame length is defined in the following as the streamwise distance between the burner exit and the farthest downstream plane normal to the flame axis that contacts a luminous region of the flame. For the present flames in coflowing air, this length was generally associated with the end of luminosity at the flame axis. For the flames of Lin et al.[4] in still air, however, this location was either along the axis or at an annular soot layer for the closed- and open-tip flames observed near laminar smoke-point conditions for nonbuoyant flames in still gases.[7]

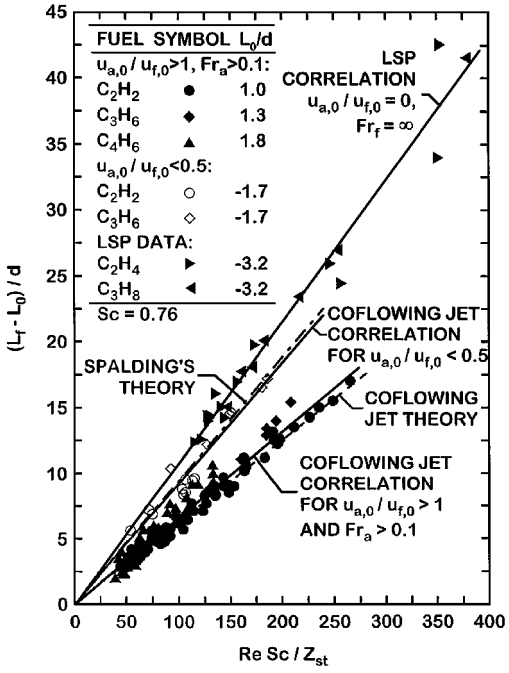


**Fig. 4 Luminous flame lengths of hydrocarbon-fueled laminar-jet diffusion flames burning in coflowing air: correlation and measurements of Lin et al.[4] for $u_{a,o}/u_{f,o}=0$, predictions of the Spalding[5] theory for $u_{a,o}/u_{f,o}=0$, correlation and measurements of the present investigation for $0.22 \le u_{a,o}/u_{f,o} < 0.5$, and correlation and measurements of the present investigation for coflowing jet theory.**

Measured and predicted lengths of flames in coflowing and still air are plotted in Fig. 4. Present measurements have been divided into two groups: 1) $u_{a,o}/u_{f,o} < 0.5$, which roughly approximates nonbuoyant flames in still air; and 2) $u_{a,o}/u_{f,o} > 1$ for $Fr_a > 0.1$, which roughly approximates nonbuoyant flames in coflowing air. All of the measurements are presented as suggested by the simplified theories of flames in coflowing and still air, e.g., Eq. (10) for flames in coflowing air, with $(L_f - L_o)/d$ plotted as a function of $Re\ Sc/Z_{st}$. Values of $Z_{st}$ used in the plots are as follows: 0.0704 for acetylene, 0.0636 for ethylene and propylene, 0.0667 for 1,3-butadiene and 0.0602 for propane. Clearly, as mentioned earlier, values of $Z_{st}$ do not vary significantly over the present test range. All other properties were obtained from Braun et al.[38] Values of $Sc$ were based on the properties of air at the mean temperatures of the flames; these values do not change significantly over the present test range so that a mean value of $Sc = 0.76$ was used for plotting all of the data. The values of $\mu$ used to find $Re$ for the plots also was based on the properties of air at the mean flame temperature. Virtual origins were selected so that fits of the measurements for various fuels and ambient flow conditions passed through the origins of the plots; the resulting values of $L_o/d$ are summarized in the legend of Fig. 4. Finally, plots of the various predictions for $C_f = 1.00$ (denoted theory) and for best-fit correlations of the various measurements (denoted correlation) are also shown on the figure. For convenience, the values of $L_o/d$ and $C_f$ for all of the flame-length plots considered here are summarized in Table 2.

The correlation of the flames in still gases according to the simple Spalding[5] analysis has already been discussed by Lin et al.[4] The results illustrated in Fig. 4 for flames in still gases represent near laminar smoke-point conditions and yield an excellent correlation having relatively little scatter with $C_f = 1.13$. As noted earlier, these luminous flame lengths for near laminar smoke-point conditions are roughly twice as long as the measurements of Sunderland et al.[8] for soot-free (blue) flames (Table 2). Present results for coflowing jet flames with $u_{a,o}/u_{f,o} > 1$ also yield a good correlation according to the simplified theory of Eq. (10), with $C_f = 1.05$ in this case. Thus, flame lengths for flames in still and coflowing gases have roughly the ratio discussed earlier in connection with Eq. (7), e.g., $L_f$ (still air)$/L_f$ (coflow) $\approx \frac{3}{2}$, with this ratio being relatively independent of $u_{a,o}/u_{f,o}$ and $Re$ in accord with the simplified theories. Finally, present results for small coflow velocities $0.22 < u_{a,o}/u_{f,o} < 0.5$ yield a reasonably good correlation in terms of the theory for flames in still gases, e.g., $C_f = 0.98$ from Table 2. These results also are in reasonably good agreement with earlier measurements in still gases, with the somewhat shorter flame lengths in the presence of slow coflow being consistent with other effects of coflow seen in Fig. 4.

**Table 2 Summary of flame-length correlations**

| Flame system | Source | $L_o/d$ | $C_f^a$ | $\sigma_{c_f}$ |
|---|---|---|---|---|
| Nonbuoyant laminar-jet diffusion flame in coflowing air ($u_{a,o}/u_{f,o} > 1$, $Fr_a > 0.1$, soot-containing flames) | Present study | 1.4[b] | 1.05 | 0.12 |
| Nonbuoyant laminar-jet diffusion flame in still air ($u_{a,o}/u_{f,o} = 0$, $Fr_f = \infty$, soot-containing flames) | Lin et al.[4] | −3.2 | 1.13 | —— |
| Nonbuoyant laminar-jet diffusion flame in slow-moving air ($0.22 \le u_{a,o}/u_{f,o} < 0.5$, soot-containing flames) | Present study | −1.7 | 0.98 | 0.10 |
| Nonbuoyant laminar-jet diffusion flame in still air ($u_{a,o}/u_{f,o} = 0$, $Fr_f = \infty$, soot-free, blue, flames) | Sunderland et al.[8] | 2.7 | 0.56 | —— |

[a]Empirical flame-length parameter based on Eq. (10) for flames in coflowing air and corresponding equations in Ref. 4 for flames in still or slow-moving ($u_{a,o}/u_{f,o} < 0.5$) air.
[b]Average of following individual values of $L_o/d$ for particular hydrocarbon fuels: 1.0 for $C_2H_2$, 1.3 for $C_3H_6$, and 1.8 for $C_4H_6$.

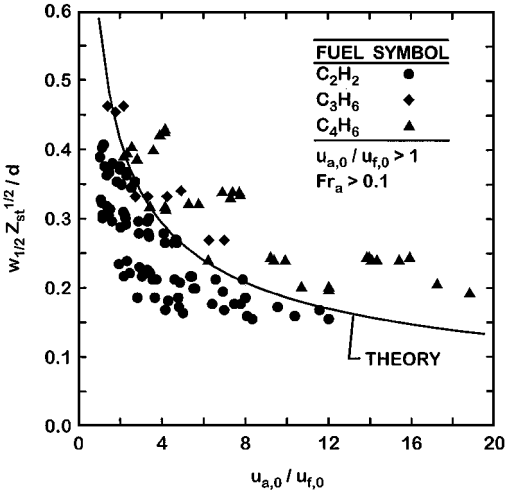


**Fig. 5 Measured and predicted luminous flame diameters of hydrocarbon-fueled laminar-jet diffusion flames burning in coflowing air at various velocity ratios for $u_{a,o}/u_{f,o} > 1$ and $Fr_a > 0.1$.**

**Flame Diameters**

The normalized characteristic flame diameter $w_{1/2}Z_{st}^{1/2}/d$ for coflowing jet diffusion flames is inversely proportional to the square root of the air/fuel velocity ratio and independent of flow transport properties, according to Eq. (9). This relationship, illustrated in Fig. 5, is based on present measurements for $u_{a,o}/u_{f,o} > 1$ and $Fr_a > 0.1$ along with the predictions of Eq. (9). The measurements follow the general trend of the predictions but are rather scattered. There also is a tendency for flame diameters to progressively increase as a function of fuel type in the order of acetylene, propylene, and 1,3-butadiene.

Insight concerning the scatter of the measurements in Fig. 5 was sought by plotting the entire argument of Eq. (9) as a function of normalized flame length, similar to the approach used for characteristic flame diameters for flames in still air by Lin et al.[4] These results are illustrated in Fig. 6 for the same range of test conditions as Fig. 5. The scatter about the predictions progressively decreases as the normalized flame length increases; therefore, small-flame aspect ratios appear to be mainly responsible for the scatter seen

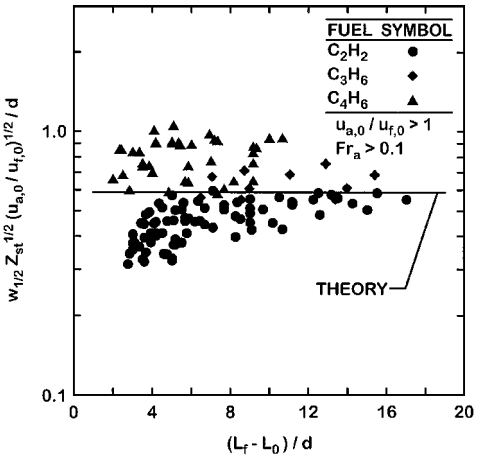


**Fig. 6 Measured and predicted luminous flame diameters of hydrocarbon-fueled laminar-jet diffusion flames burning in coflowing air at various flame lengths for $u_{a,o}/u_{f,o} > 1$ and $Fr_a > 0.1$.**

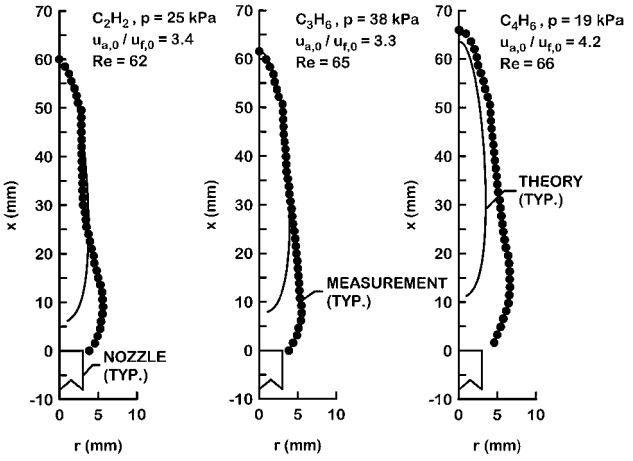


**Fig. 7 Measured and predicted luminous flame shapes for acetylene-, propylene-, and 1,3-butadiene-fueled laminar-jet diffusion flames burning in coflowing air.**

in Fig. 5. The normalized flame diameters illustrated in Fig. 6 also progressively increase as a function of fuel type in the order of acetylene, propylene, and 1,3-butadiene. Similar increases of normalized flame diameters also were observed when changing from ethylene- to propane-fueled flames in still gases.[4] The reasons for these fuel effects are not known, but fortunately the effects are not very large in view of the approximations of the simplified theories.

### Flame Shapes

Measured and predicted luminous flame shapes are compared as the final step in the evaluation of the simplified flame-shape analysis leading to Eqs. (9–12) for flames in coflowing air. This comparison was carried out for relatively large flame lengths (or large aspect ratios) to reduce problems of flame-width predictions at small-flame aspect ratios discussed in connection with Figs. 5 and 6. Typical results for acetylene-, propylene-, and 1,3-butadiene-fueled flames at similar Reynolds numbers (*Re* of 62–66) and air/fuel velocity ratios ($u_{a,o}/u_{f,o}$ of 3.3–4.2) are illustrated in Fig. 7. Flame radius is plotted as a function of streamwise distance to illustrate directly the effectiveness of flame-shape predictions. The predictions clearly are quite good in the far field. A minor exception is a tendency for predictions to underestimate the radius of the 1,3-butadiene-fueled flame in the far field, similar to the results discussed in connection with Fig. 6. The far-field approximations of the analysis, however, break down near the nozzle exit where the predictions are not very satisfactory.

Effects of air/fuel velocity ratios and Reynolds numbers on discrepancies between measured and predicted flame shapes can

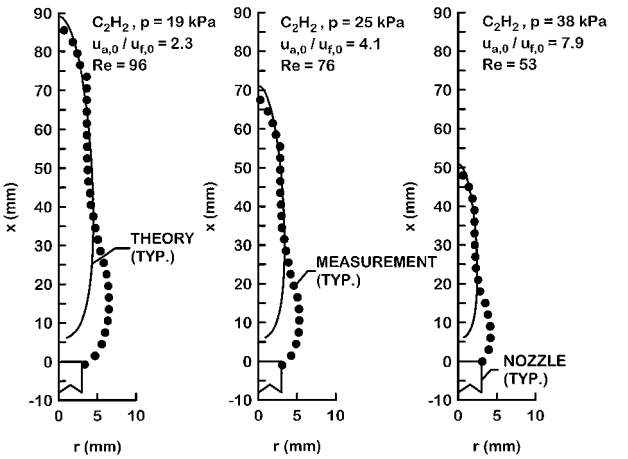


**Fig. 8 Measured and predicted luminous flame shapes for acetylene-fueled laminar-jet diffusion flames burning in coflowing air at various fuel jet and coflow conditions.**

be seen from the results plotted in Fig. 8. Conditions were selected for the plots to provide progressively shorter and narrower flames, e.g., acetylene-fueled flames having $u_{a,o}/u_{f,o} = 2.3$, 4.1, and 7.9 and $Re = 96$, 76, and 53, respectively. The approximate analysis is seen to provide good predictions of trends with respect to variations of air/fuel velocity ratios and Reynolds numbers in the far field. Predictions near the source, however, are not satisfactory because of the failure of the far-field approximations. Mahalingam et al.[35] observe similar trends where predictions are not satisfactory near the source when comparing their approximate self-similar analysis with the exact results of the Burke and Schumann[2] analysis for the property approximations and the uniform velocity flame conditions that they consider.

## Conclusions

The luminous flame shapes of steady, nonbuoyant, round hydrocarbon-fueled laminar-jet diffusion flames burning in coflowing air were studied both experimentally and theoretically. Test conditions involved acetylene-, propylene-, and 1,3-butadiene-fueled flames having initial reactant temperatures of 300 K, ambient pressures of 19–50 kPa, jet-exit Reynolds numbers of 18–121, and initial air/fuel velocity ratios of 0.22–32.45 to yield luminous flame lengths of 21–108 mm. The present test flames usually were close to the laminar smoke point but were not soot emitting. The new measurements were used to evaluate predictions of luminous flame shapes based on simplified analysis due to Spalding[5] and Mahalingam et al.[35] The major conclusions of the study are as follows:

1) The present extension of the simplified analysis of nonbuoyant round laminar-jet diffusion flames in coflow due to Mahalingam et al.[35] provided reasonably good predictions of the luminous shapes of the present flames in the far field for $u_{a,o}/u_{f,o} > 1$ and $Fr_a > 0.1$ after appropriate selections of empirical flame-length parameters, e.g., $L_o/d$ and $C_f$. The predictions were most satisfactory for large aspect ratio flames and tended to fail near the source where the far-field approximations used in the analysis were no longer valid.

2) The simplified analysis of nonbuoyant laminar-jet diffusion flames in still air due to Spalding,[5] developed by Lin et al.,[4] provided reasonably good predictions of the luminous shapes of the present flames in slow-moving coflow for $0.22 \leq u_{a,o}/u_{f,o} < 0.5$ after appropriate selections of empirical flame-length parameters, e.g., $L_o/d$ and $C_f$. Present values of the flame lengths (or $C_f$) for slow coflow ($u_{a,o}/u_{f,o} < 0.5$) were 15% smaller than the earlier results of Lin et al.[4] with no coflow because of enhanced mixing rates caused by coflow.

3) Based on present correlations of the luminous flame boundaries of nonbuoyant laminar-jet diffusion flames in still and coflowing air, luminous flame lengths increase linearly with fuel flow rates but are relatively independent of jet-exit diameter, pressure, and air/fuel velocity ratio (for flames in coflow). Nevertheless flames in still air are roughly 50% longer than flames in significant coflow ($u_{a,o}/u_{f,o} > 1$) at comparable conditions, with this difference being

relatively independent of air/fuel velocity ratio and jet-exit Reynolds number.

4) Based on present correlations of the luminous flame boundaries of nonbuoyant laminar-jet diffusion flames in still and coflowing air, characteristic luminous flame diameters vary linearly with jet-exit diameter and are relatively independent of flow physical properties and jet-exit Reynolds numbers. For flames having significant levels of coflow ($u_{a,o}/u_{f,o} > 1$), however, characteristic luminous flame diameters are also inversely proportional to the square root of $u_{a,o}/u_{f,o}$. Thus, large aspect ratio flames can best be achieved using small injector diameters, large injector Reynolds numbers, and large air/fuel velocity ratios, subject to laminar smoke-point limitations if nonsooting flames are desired.

5) Progressive increases of luminous flame lengths at comparable conditions were observed as the laminar smoke point was approached for nonbuoyant laminar-jet diffusion flames in coflowing air. This behavior was similar to the observations of Lin et al.[4] that the luminous lengths of nonbuoyant laminar-jet diffusion flames in still air were roughly twice as long at near laminar smoke-point conditions as soot-free (blue) flames at comparable conditions. Whether quantitative effects of approach to the laminar smoke point are the same for flames in coflowing and still air, however, still must be established.

Finally, we recommend that the correlation of flame shapes for nonbuoyant laminar-jet diffusion flames in coflowing air [Eqs. (9–12)] be used with caution outside the present test range and until the results are definitively confirmed for long-term microgravity conditions where the intrusion of effects of transient flame development and buoyancy are absent. In particular, past observations of the shapes of steady nonbuoyant laminar-jet diffusion flames in still gases based on space-based observations in microgravity generally have been found to differ from earlier measurements obtained using ground-based facilities due to effects of transient flame development and disturbances due to buoyancy. The present conclusions concerning effects of burner diameter follow from the simplified theory; experimental evaluation of these trends is needed.

## Acknowledgments

This research was supported by NASA Grants NAG3-1245 and NAG3-2048 under the technical management of David L. Urban of the NASA Lewis Research Center and by Office of Naval Research Grant N00016-95-0238 under the technical management of Gabriel D. Roy.

## References

[1]Bilger, R. W., "Reaction Rates in Diffusion Flames," *Combustion and Flame*, Vol. 30, No. 3, 1977, pp. 277–284.

[2]Burke, S. P., and Schumann, T. E. W., "Diffusion Flames," *Industrial and Engineering Chemistry*, Vol. 20, No. 10, 1928, pp. 998–1004.

[3]Law, C. K., and Faeth, G. M., "Opportunities and Challenges of Combustion in Microgravity," *Progress in Energy and Combustion Sciences*, Vol. 20, No. 1, 1994, pp. 65–113.

[4]Lin, K.-C., Faeth, G. M., Sunderland, P. B., Urban, D. L., and Yuan, Z.-G., "Shapes of Nonbuoyant Round Luminous Hydrocarbon/Air Laminar Jet Diffusion Flames," *Combustion and Flame*, Vol. 116, No. 3, 1999, pp. 415–431.

[5]Spalding, D. B., *Combustion and Mass Transfer*, Pergamon, New York, 1979, pp. 185–195.

[6]Kuo, K. K., *Principles of Combustion*, Wiley, New York, 1986, pp. 360–370.

[7]Urban, D. L., Yuan, Z.-G., Sunderland, P. B., Linteris, G. T., Voss, J. E., Lin, K.-C., Dai, Z., Sun, K., and Faeth, G. M., "Structure and Soot Properties of Nonbuoyant Ethylene/Air Laminar Jet Diffusion Flames," *AIAA Journal*, Vol. 36, No. 8, 1998, pp. 1346–1360.

[8]Sunderland, P. B., Mendelson, B. J., Yuan, Z.-G., and Urban, D. L., "Shapes of Buoyant and Nonbuoyant Laminar Jet Diffusion Flames," *Combustion and Flame*, Vol. 116, No. 3, 1999, pp. 376–386.

[9]Sunderland, P. B., Mortazavi, S, Faeth, G. M., and Urban, D. L., "Laminar Smoke Points of Nonbuoyant Jet Diffusion Flames," *Combustion and Flame*, Vol. 96, No. 1, 1994, pp. 97–103.

[10]Schug, K. P., Manheimer-Timnat, Y., Yaccarino, P., and Glassman, I., "Sooting Behavior of Gaseous Hydrocarbon Diffusion Flames and the Influence of Additives," *Combustion Science and Technology*, Vol. 22, No. 5/6, 1980, pp. 235–250.

[11]Gomez, A., Sidebotham, G., and Glassman, I., "Sooting Behavior in Temperature-Controlled Laminar Diffusion Flames," *Combustion and Flame*, Vol. 58, No. 1, 1984, pp. 45–57.

[12]Mitchell, R. E., Sarofim, A. F., and Clomberg, L. A., "Experimental and Numerical Investigation of Confined Laminar Diffusion Flames," *Combustion and Flame*, Vol. 37, No. 3, 1980, pp. 227–244.

[13]Saito, K., Williams, F. A., and Gordon, A. S., "Structure of Laminar Coflow Methane-Air Diffusion Flames," *Journal of Heat Transfer*, Vol. 108, No. 3, 1986, pp. 640–648.

[14]Saito, K., Williams, F. A., and Gordon, A. S., "Effects of Oxygen on Soot Formation in Diffusion Flames," *Combustion Science and Technology*, Vol. 47, No. 3/4, 1986, pp. 117–138.

[15]Sunderland, P. B., "Soot Nucleation and Growth in Weakly Buoyant Laminar Jet Diffusion Flames," Ph.D. Dissertation, Dept. of Aerospace Engineering, Univ. of Michigan, Ann Arbor, MI, June 1995.

[16]Sunderland, P. B., Köylü, Ü. Ö., and Faeth, G. M., "Soot Formation in Weakly Buoyant Acetylene-Fueled Laminar Jet Diffusion Flames Burning in Air," *Combustion and Flame*, Vol. 100, No. 1/2, 1995, pp. 310–322.

[17]Lin, K.-C., "Hydrodynamic Effects on Soot Formation in Laminar Hydrocarbon-Fueled Diffusion Flames," Ph.D. Dissertation, Dept. of Aerospace Engineering, Univ. of Michigan, Ann Arbor, MI, June 1996.

[18]Lin, K.-C., Sunderland, P. B., and Faeth, G. M., "Soot Nucleation and Growth in Acetylene/Air Laminar Coflowing Jet Diffusion Flames," *Combustion and Flame*, Vol. 104, No. 3, 1996, pp. 369–375.

[19]Lin, K.-C., and Faeth, G. M., "Hydrodynamic Suppression of Soot Emissions in Laminar Diffusion Flames," *Journal of Propulsion and Power*, Vol. 12, No. 1, 1996, pp. 10–17.

[20]Cochran, T. H., and Masica, W. J., "An Investigation of Gravity Effects on Laminar Gas Jet Diffusion Flames," *Thirteenth Symposium (International) on Combustion*, Combustion Inst., Pittsburgh, PA, 1970, pp. 821–829.

[21]Haggard, J. B., Jr., and Cochran, T. H. "Stable Hydrocarbon Diffusion Flames in a Weightless Environment," *Combustion Science and Technology*, Vol. 5, No. 4–6, 1972, pp. 291–298.

[22]Edelman, R. B., Fortune, O. F., Weilerstein, G., Cochran, T. H., and Haggard, J. B., Jr., "An Analytical and Experimental Investigation of Gravity Effects upon Laminar Gas Jet-Diffusion Flames," *Fourteenth Symposium (International) on Combustion*, Combustion Inst., Pittsburgh, PA, 1972, pp. 399–412.

[23]Edelman, R. B., and Bahadori, M. Y., "Effects of Buoyancy on Gas-Jet Diffusion Flames: Experiment and Theory," *Acta Astronautica*, Vol. 13, No. 11/12, 1986, pp. 681–688.

[24]Bahadori, M. Y., Edelman, R. B., Stocker, D. P., and Olson, S. L., "Ignition and Behavior of Laminar Gas-Jet Diffusion Flames in Microgravity," *AIAA Journal*, Vol. 28, No. 2, 1990, pp. 236–244.

[25]Bahadori, M. Y., Stocker, D. P., and Edelman, R. B., "Effects of Pressure on Microgravity Hydrocarbon Diffusion Flames," AIAA Paper 90-0651, Jan. 1990.

[26]Bahadori, M. Y., Edelman, R. B., Sotos, R. G., and Stocker, D. P., "Radiation from Gas-Jet Diffusion Flames in Microgravity Environments," AIAA Paper 91-0719, Jan. 1991.

[27]Bahadori, M. Y., Edelman, R. B., Stocker, D. P., Sotos, R. G., and Vaughan, D. F., "Effects of Oxygen Concentration on Radiative Loss from Normal-Gravity and Microgravity Methane Diffusion Flames," AIAA Paper 92-0243, Jan. 1992.

[28]Jost, W., *Explosion and Combustion Processes in Gases*, McGraw–Hill, New York, 1946, Chap. 1.

[29]Roper, F. G., "Prediction of Laminar Jet Diffusion Flames; Part I: Theoretical Model," *Combustion and Flame*, Vol. 29, No. 3, 1977, pp. 219–226.

[30]Roper, F. G., Smith, C., and Cunningham, A. C., "The Predictions of Laminar Jet Diffusion Flame Sizes: Part II. Experimental Verification," *Combustion and Flame*, Vol. 29, No. 3, 1977, pp. 227–234.

[31]Klajn, M., and Oppenheim, A. K., "Influence of Exothermicity on the Shape of a Diffusion Flame," *Nineteenth Symposium (International) on Combustion*, Combustion Inst., Pittsburgh, PA, 1982, pp. 223–235.

[32]Li, S. C., Gordon, A. S., and Williams, F. A., "A Simplified Method for the Computation of Burke-Schumann Flames in Infinite Atmospheres," *Combustion Science and Technology*, Vol. 104, No. 1–3, 1995, pp. 75–91.

[33]Ban, H., Venkatesh, S., and Saito, K., "Convection-Diffusion Controlled Laminar Micro Flames," *Journal of Heat Transfer*, Vol. 116, No. 4, 1994, pp. 954–959.

[34]Williams, F. A., *Combustion Theory*, 2nd ed., Benjamin/Cummings Publishing, Menlo Park, CA, 1985, pp. 38–47.

[35]Mahalingam, S., Ferziger, J. H., and Cantwell, B. J., "Self-Similar Diffusion Flames," *Combustion and Flame*, Vol. 82, No. 2, 1990, pp. 231–234.

[36]Hamins, A., Gordon, A. S., Saito, K., and Seshadri, K., "Acetone Impurity in Acetylene from Tanks," *Combustion Science and Technology*, Vol. 45, No. 5, 1986, pp. 309–310.

[37]Schlichting, H., *Boundary Layer Theory*, 4th ed., McGraw–Hill, New York, 1960, pp. 160–164.

[38]Braun, W. G., Danner, R. P., and Daubert, T. E., *Technical Data Book—Petroleum Refining*, 3rd ed., American Petroleum Inst., Washington, DC, 1976, Chaps. 11 and 13.

S. K. Aggarwal
*Associate Editor*